Electronic Supplementary Material (ESI) for Nanoscale.

Supporting Information

Surface Reconstruction of AgPd Nanoalloy Particles during Electrocatalytic Formate Oxidation Reaction†

Longfei Guo, [a,b] *Fuyi Chen,* [*a,b] *Tao Jin,* [a,b] *Huazhen Liu,* [b] *Nan Zhang,* [a] *Yachao Jin,* [a,b] *Qiao Wang,* [a,b] *Quan Tang,* [a,b] *Bowei Pan* [b]

[a]State Key Laboratory of Solidification Processing, Northwestern Polytechnical University, Xi'an 710072, China

[b]School of Materials Science and Engineering, Northwestern Polytechnical University, Xi'an, 710072, China

[*]Corresponding author: E-mail: fuyichen@nwpu.edu.cn

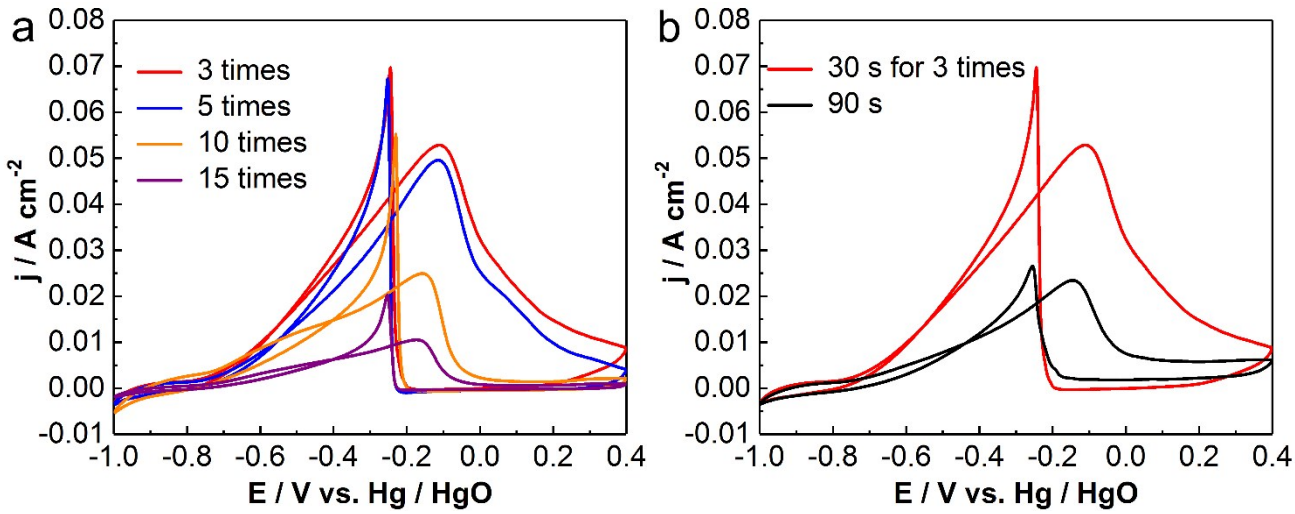

Fig. S1. CV curves of AgPd/rGO catalysts prepared with different microwave heating parameters. (a) CV curves of AgPd/rGO prepared with heated at 800 W for 30 s, then stirred for 5 s, and repeated for 3, 5, 10 and 15 times. (b) CV curves of AgPd/rGO catalysts prepared with heated under 800 W for 30 s, then stirred for 5 s, and repeated for 3 times (the red line), compared with continuous heating for 90 s (the black line). All of the CV curves were recorded in N_2-saturated 1 M KOH + 1 M HCOOK electrolyte at a scan rate of 50 mV s^{-1} and normalized with the area of glassy carbon (GC) electrode (0.196 cm^2).

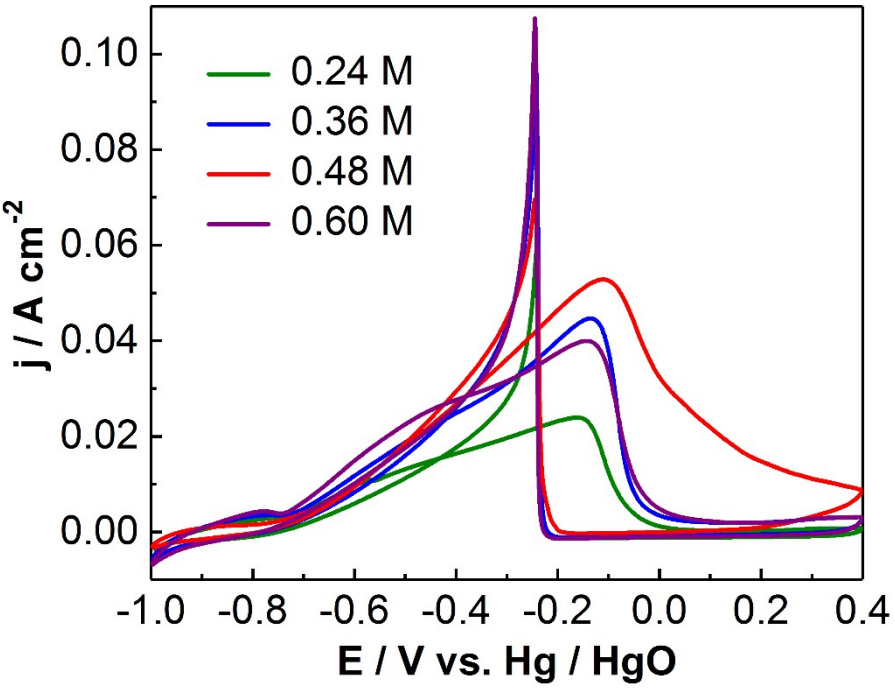

Fig. S2. CV curves of AgPd/rGO catalysts prepared with different trisodium citrate concentration of 0.24 M, 0.36 M, 0.48 M and 0.60 M recorded in N_2-saturated 1 M KOH + 1 M HCOOK electrolyte at a scan rate of 50 mV s^{-1} normalized with the area of GC electrode (0.196 cm^2).

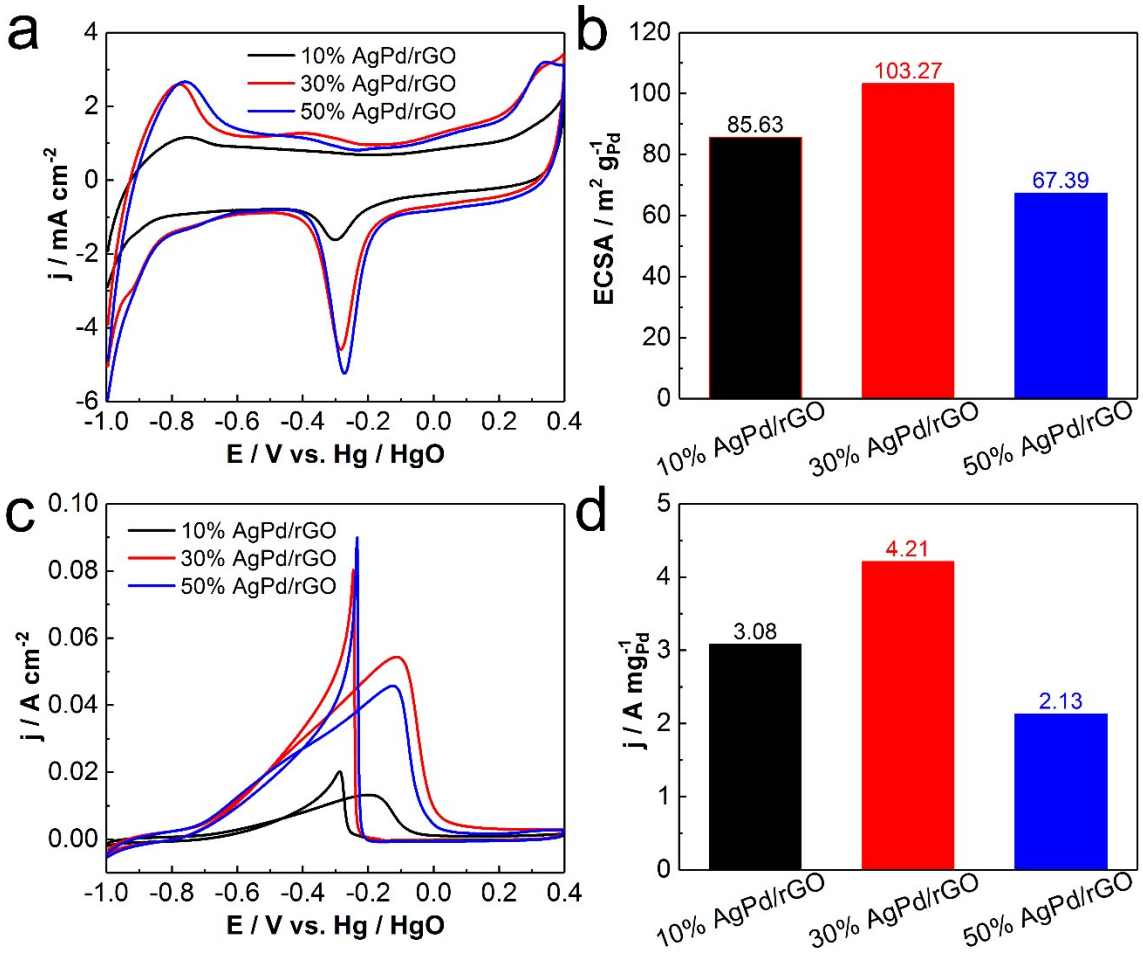

Fig. S3. (a) CV curves of AgPd/rGO catalysts with the metal loading of 10%, 30% and 50% recorded in 1 M KOH electrolyte normalized with the area of GC electrode. (b) ECSAs of AgPd/rGO catalysts with the metal loading of 10%, 30% and 50%. (c) CV curves for FOR of AgPd/rGO catalysts with the metal loading of 10%, 30% and 50% recorded in 1 M KOH + 1 M HCOOK electrolyte. (d) FOR peak mass activity of AgPd/rGO catalysts with the metal loading of 10%, 30% and 50%. Unless indicated, all of the CV curves were recorded with a scan rate of 50 mV s^{-1}.

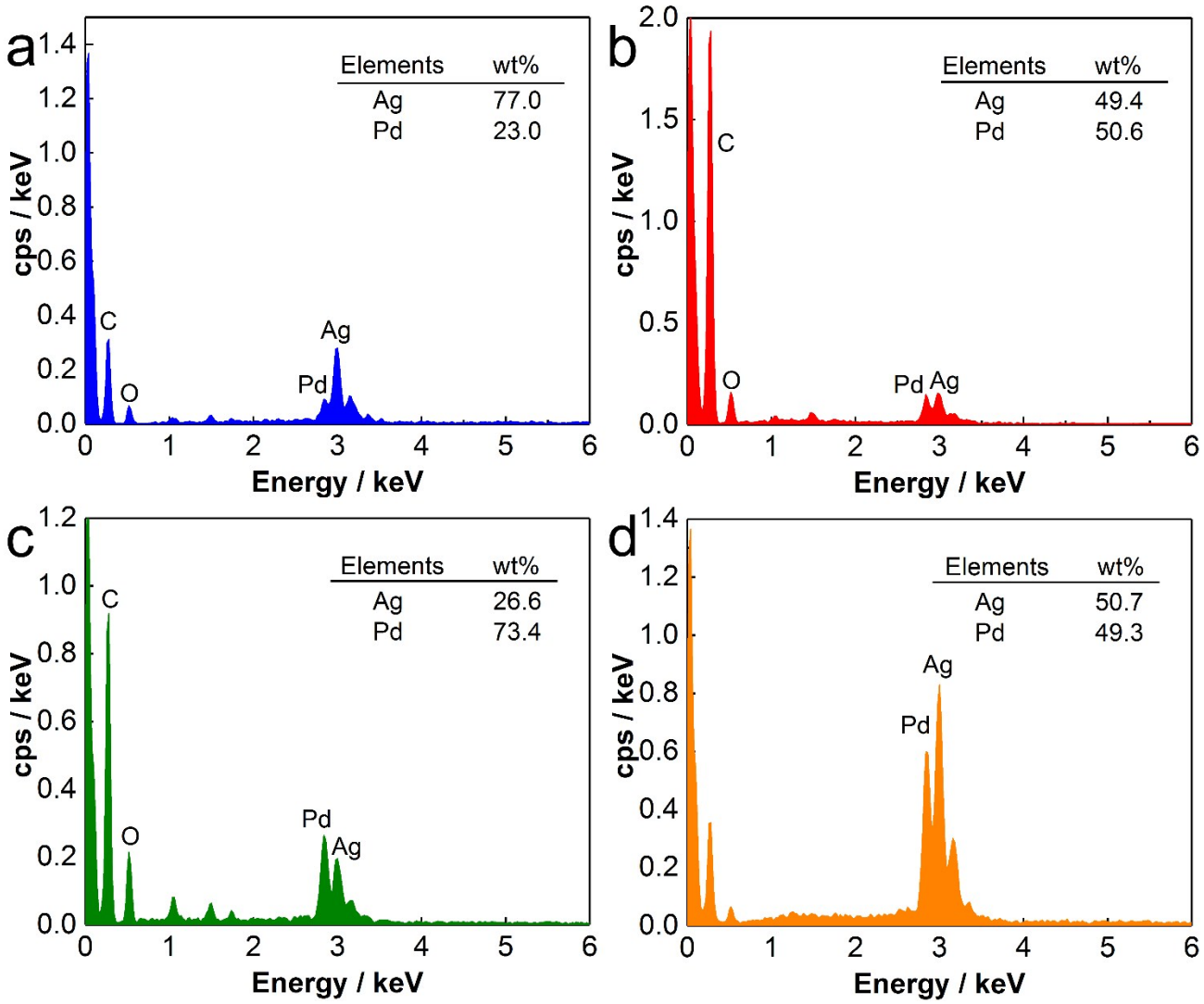

Fig. S4 SEM-EDS of (a) $Ag_{77}Pd_{23}$/rGO, (b) $Ag_{49}Pd_{51}$/rGO, (c) $Ag_{27}Pd_{73}$/rGO and (d) $Ag_{51}Pd_{49}$ nanoalloy catalysts.

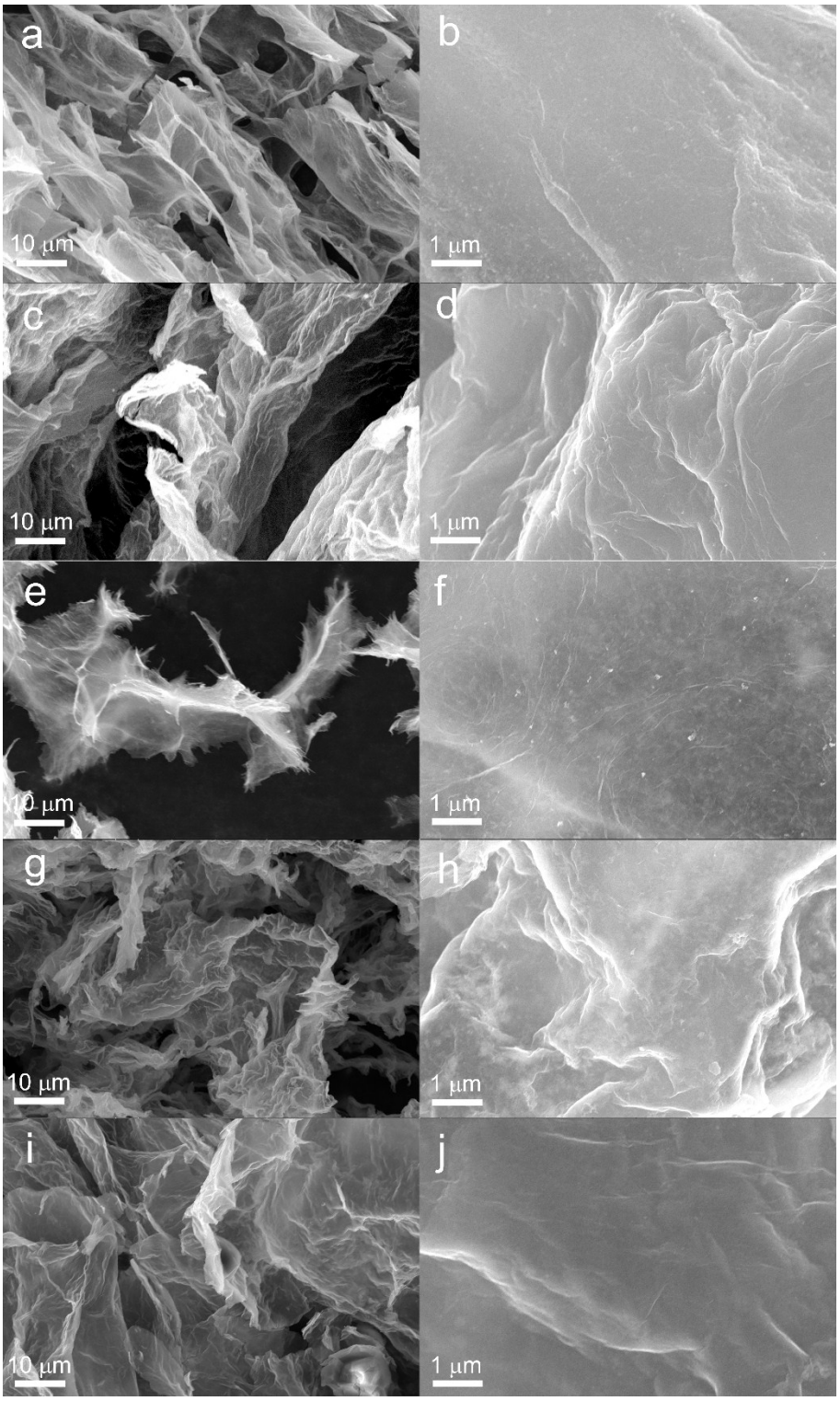

Fig. S5. SEM images of (a, b) Ag/rGO, (c, d) $Ag_{77}Pd_{23}$/rGO, (e, f) $Ag_{49}Pd_{51}$/rGO, (g, h) $Ag_{27}Pd_{73}$/rGO and (i, j) Pd/rGO catalysts.

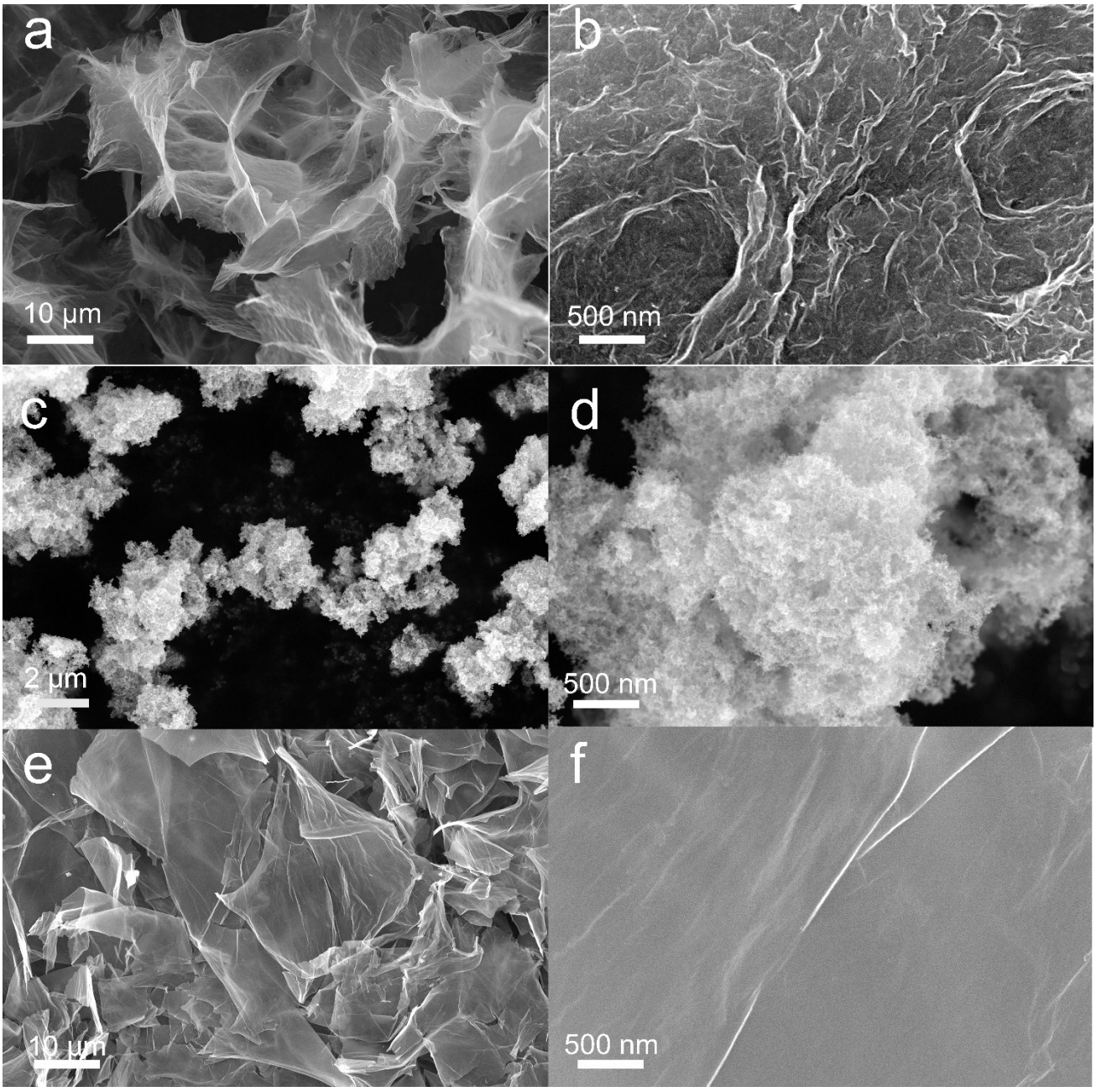

Fig. S6. SEM images of (a, b) $Ag_{49}Pd_{51}$/rGO, (c, d) $Ag_{51}Pd_{49}$ nanoalloy, and (e, f) Reduced graphene oxide (rGO) catalysts.

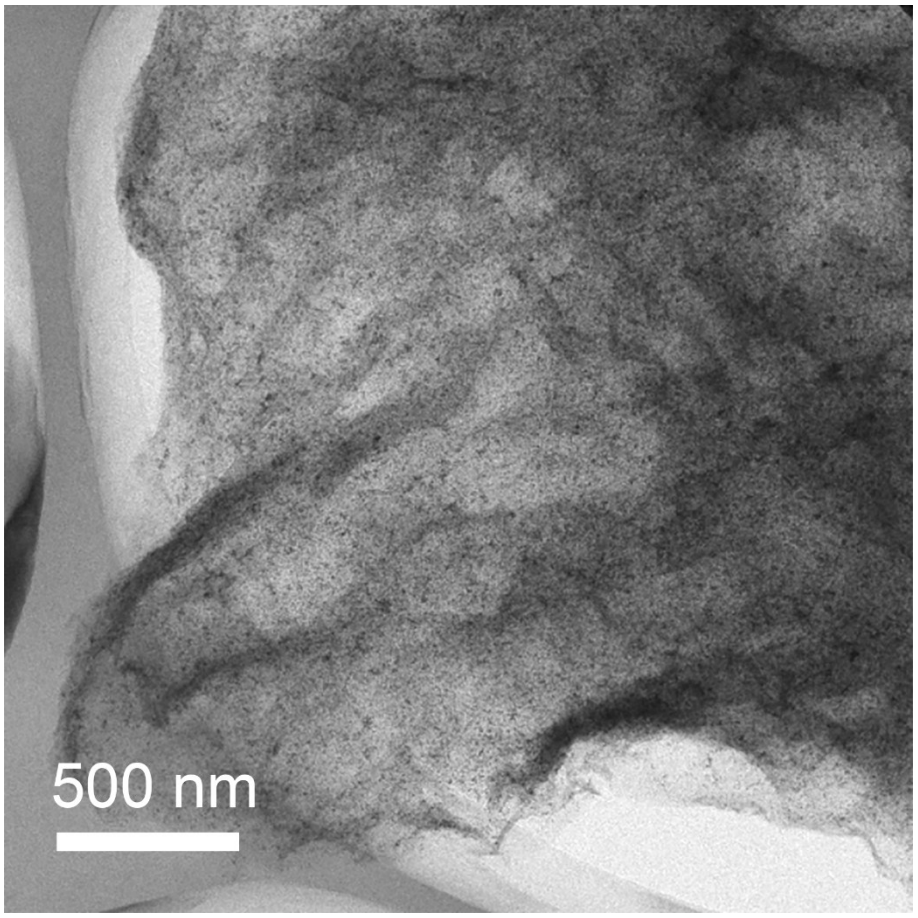

Fig. S7. TEM image of $Ag_{49}Pd_{51}$/rGO catalyst.

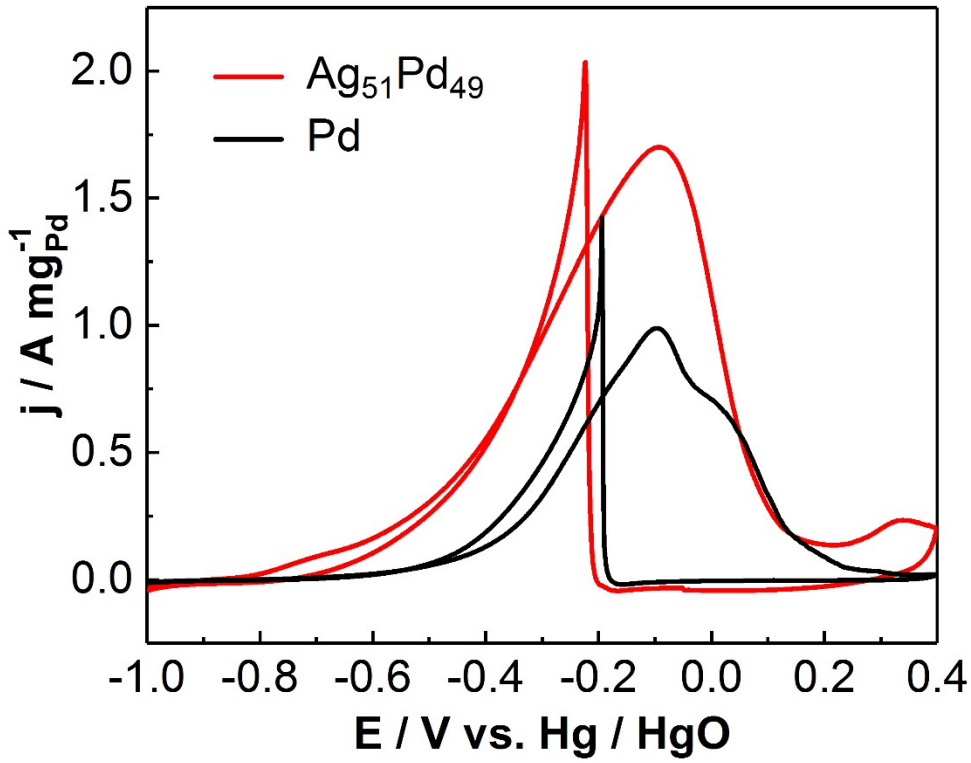

Fig. S8. CV curves of $Ag_{51}Pd_{49}$ nanoalloy and monometallic Pd catalysts recorded in N_2-saturated 1 M KOH + 1 M HCOOK electrolyte at a scan rate of 50 mV s^{-1}. The more negative formate oxidation onset potential and higher current density of $Ag_{51}Pd_{49}$ nanoalloy than monometallic Pd demonstrate the alloying effect of Ag with Pd on improving FOR catalytic activity of Pd catalyst.

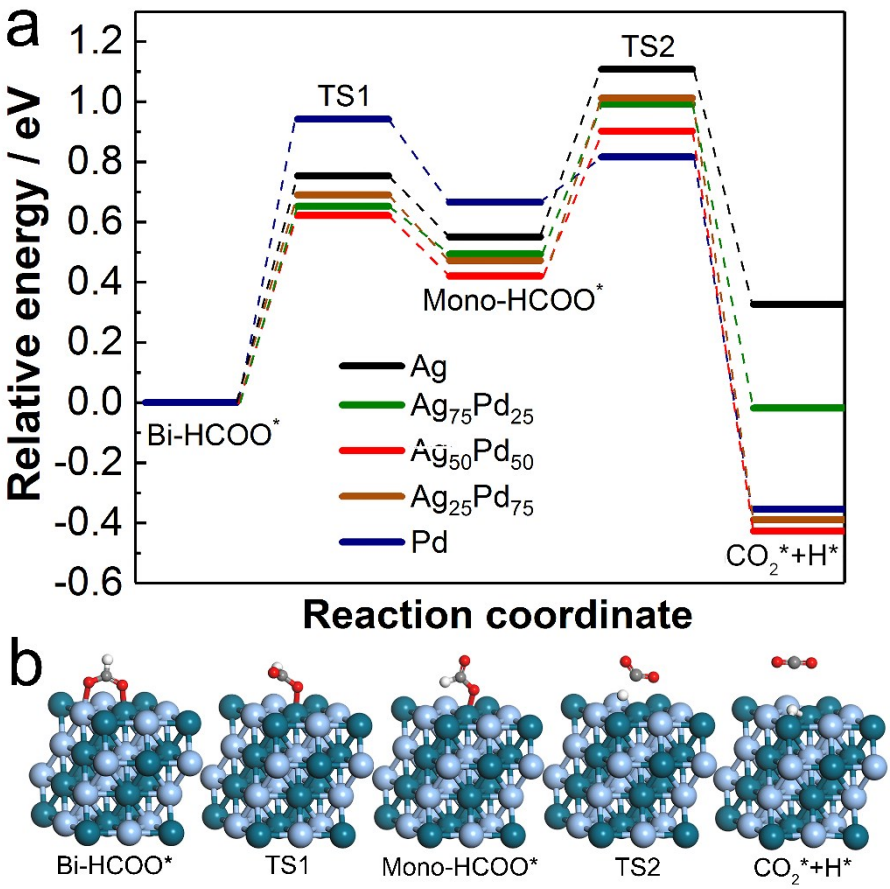

Fig. S9. (a) Potential energy profiles for $HCOO^-$ oxidation on various AgPd alloy, pure Ag and pure Pd surfaces. (b) Optimized configurations (side view) of the initial state (Bi-$HCOO^*$), transition state 1 (TS1), Intermediate state (Mono-$HCOO^*$), transition state 2 (TS2) and final state ($CO2^*$ + H^*) for $Ag_{50}Pd_{50}$ (111) surface. C, O, H, Ag and Pd atoms are indicated in gray, red, white, light-blue and dark-blue, respectively. The oxidation of $HCOO^-$ on Ag (111) plane requires 0.33 eV of energy in total, which is thermodynamically unfavorable, while the process on $Ag_{75}Pd_{25}$, $Ag_{50}Pd_{50}$, $Ag_{25}Pd_{75}$ and Pd (111) planes release 0.02, 0.43, 0.39, and 0.35 eV, respectively. Among them, the oxidation of $HCOO^-$ on $Ag_{50}Pd_{50}$ (111) plane releases the highest energy, proving the thermodynamically advantage of $Ag_{50}Pd_{50}$ on catalyzing FOR. Moreover, the maximum activation energy of $HCOO^-$ oxidation on Ag, $Ag_{75}Pd_{25}$, $Ag_{50}Pd_{50}$, $Ag_{25}Pd_{75}$ and Pd

(111) planes are 0.75, 0.65, 0.62, 0.69 and 0.94 eV, respectively. Obviously, $Ag_{50}Pd_{50}$ (111) plane requires the minimum activation energy to catalyze FOR, which is kinetically more favorable. Therefore, $Ag_{50}Pd_{50}$ should exhibit the best performance for catalyzing FOR.

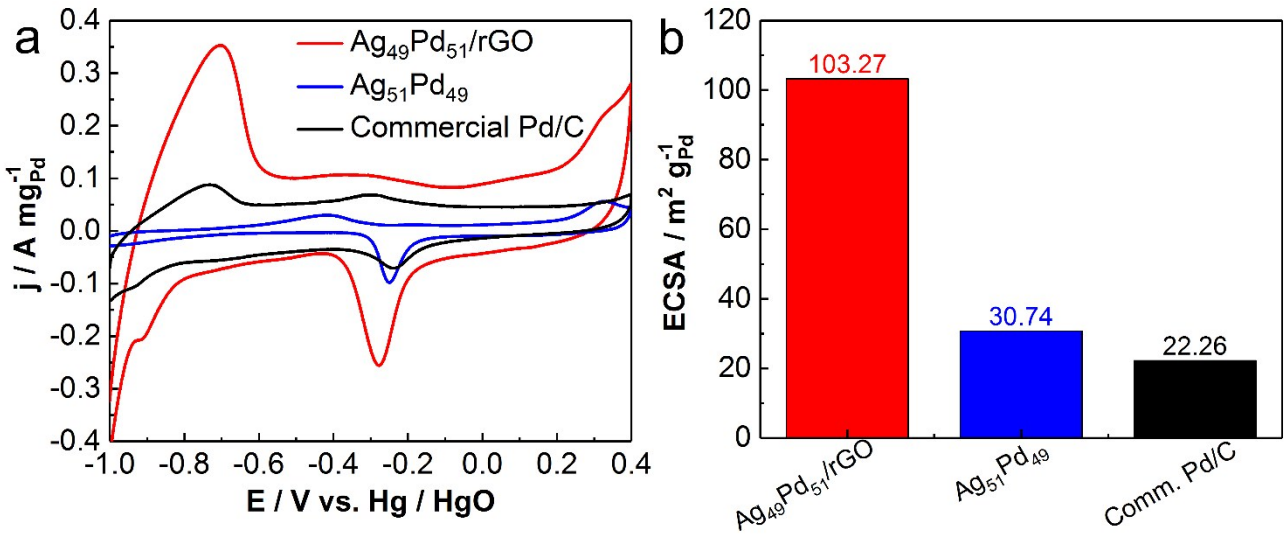

Fig. S10. (a) CV curves of $Ag_{49}Pd_{51}$/rGO, $Ag_{51}Pd_{49}$ and commercial Pd/C catalysts in N_2-saturated 1 M KOH + 1 M HCOOK electrolyte. (b) ECSAs of $Ag_{49}Pd_{51}$/rGO, $Ag_{51}Pd_{49}$ and commercial Pd/C catalysts.

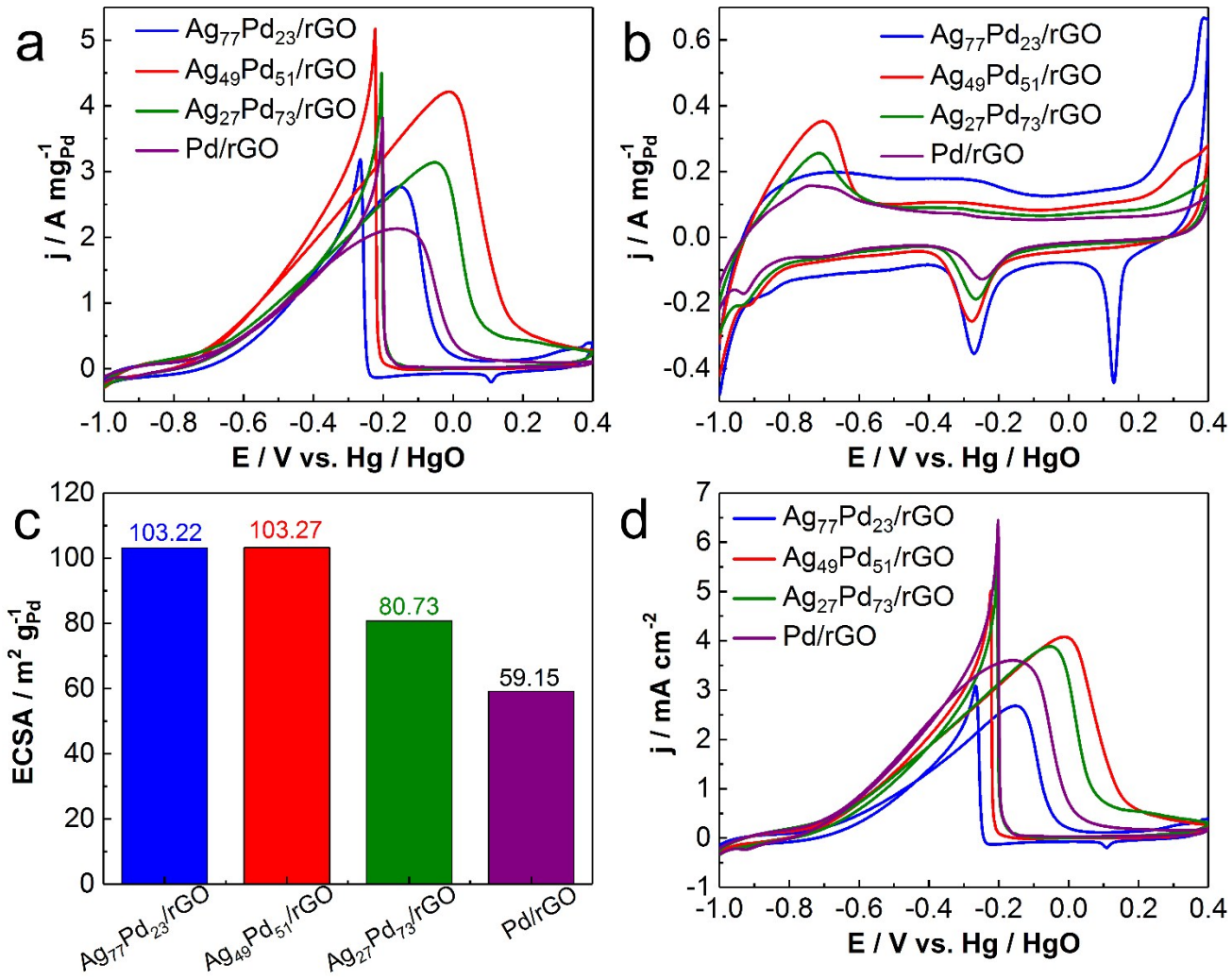

Fig. S11. (a) CV curves of $Ag_{77}Pd_{23}$/rGO, $Ag_{49}Pd_{51}$/rGO, $Ag_{27}Pd_{73}$/rGO and Pd/rGO catalysts recorded in N_2-saturated 1 M KOH + 1 M HCOOK electrolyte. (b) CV curves of $Ag_{77}Pd_{23}$/rGO, $Ag_{49}Pd_{51}$/rGO, $Ag_{27}Pd_{73}$/rGO and Pd/rGO catalysts recorded in N_2-saturated 1 M KOH electrolyte. (c) ECSAs of $Ag_{77}Pd_{23}$/rGO, $Ag_{49}Pd_{51}$/rGO, $Ag_{27}Pd_{73}$/rGO and Pd/rGO catalysts. (d) CV curves of $Ag_{77}Pd_{23}$/rGO, $Ag_{49}Pd_{51}$/rGO, $Ag_{27}Pd_{73}$/rGO and Pd/rGO catalysts recorded in N_2-saturated 1 M KOH + 1 M HCOOK electrolyte normalized with ECSAs. All of the CV curves were obtained at a scan rate of 50 mV s^{-1}.

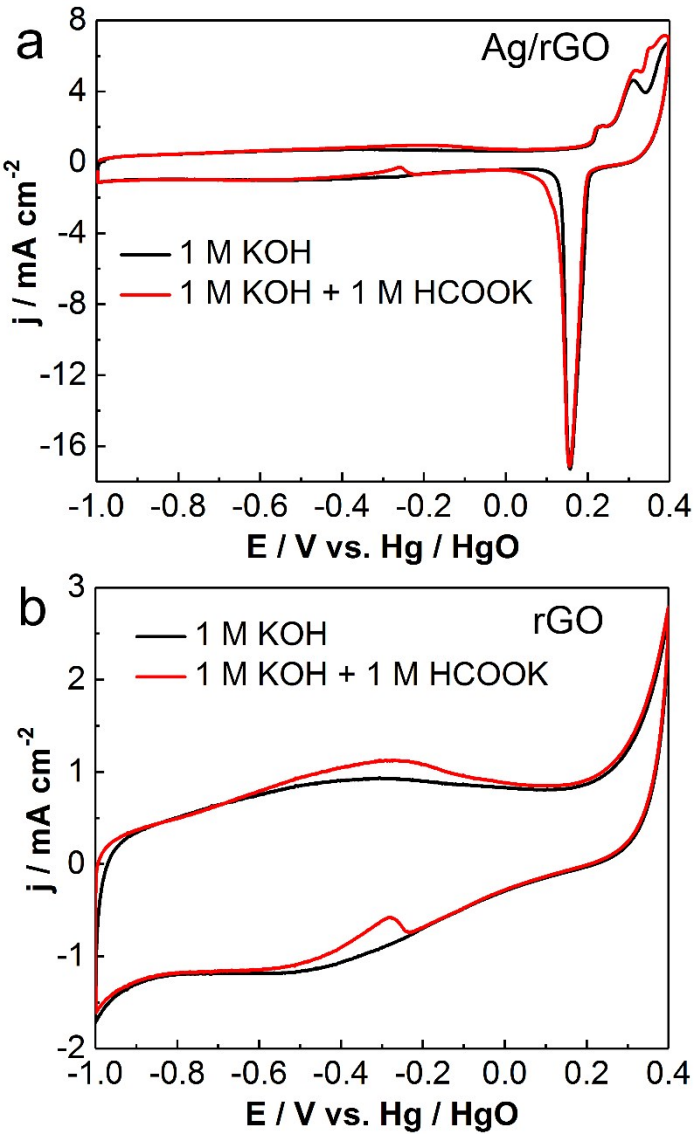

Fig. S12. CV curves of (a) Ag/rGO and (b) rGO catalysts recorded in N_2-saturated 1 M KOH and 1 M KOH + 1 M HCOOK electrolyte at a scan rate of 50 mV s^{-1} normalized with the area of glassy carbon (GC) electrode (0.196 cm^2).

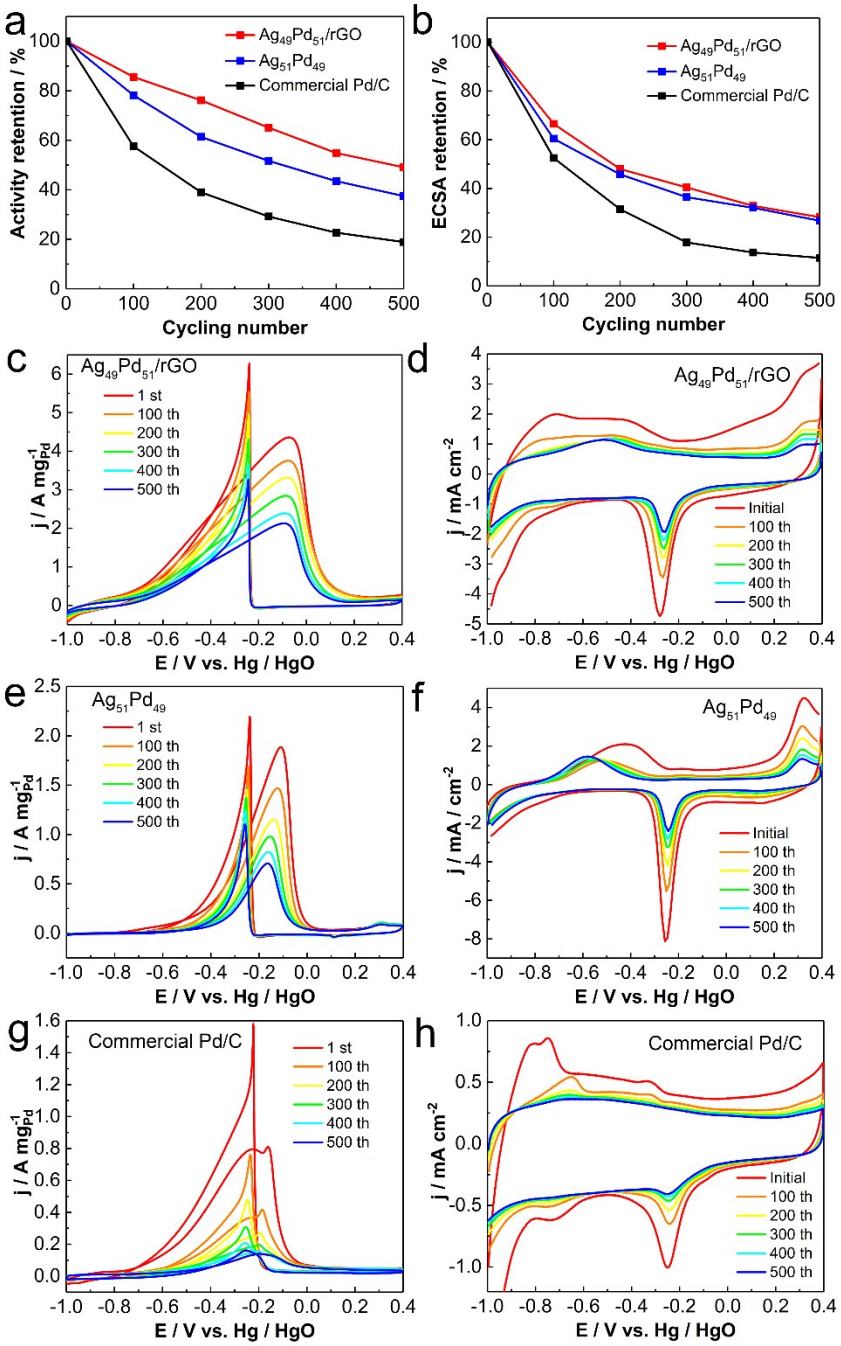

Fig. S13. (a) The percentage of retaining activity as a function of cycling number for as-prepared $Ag_{49}Pd_{51}$/rGO catalyst, unsupported $Ag_{51}Pd_{49}$ nanoalloys and commercial Pd/C catalyst. (b) The percentage of retaining ECSA as a function of cycling number for as-prepared $Ag_{49}Pd_{51}$/rGO catalyst, unsupported $Ag_{51}Pd_{49}$ nanoalloys, and commercial Pd/C catalyst. (c, e, g) CV curves of as-prepared $Ag_{49}Pd_{51}$/rGO catalyst, unsupported $Ag_{51}Pd_{49}$ nanoalloys and commercial Pd/C

catalyst at the 1 st, 100 th, 200 th, 300 th, 400 th and 500 th cycle. (d, f, h) CV curves of as-prepared $Ag_{49}Pd_{51}$/rGO catalyst, unsupported $Ag_{51}Pd_{49}$ nanoalloys and commercial Pd/C catalyst before and after 100, 200, 300, 400 and 500 cycles normalized with the area of GC electrode. All of the CV curves were obtained at a scan rate of 50 mV s^{-1}.

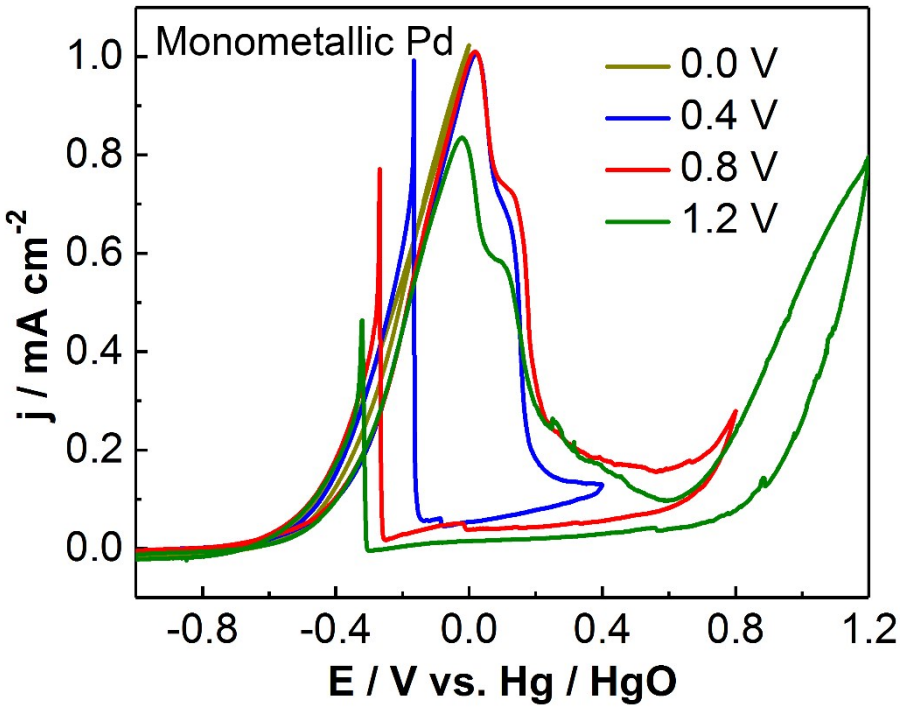

Fig. S14. CV curves of monometallic Pd catalyst recorded in N_2-saturated 1 M KOH + 1 M HCOOK electrolyte under different upper limit potential of 0.0, 0.4, 0.8 and 1.2 V at a scan rate of 50 mV s^{-1}.

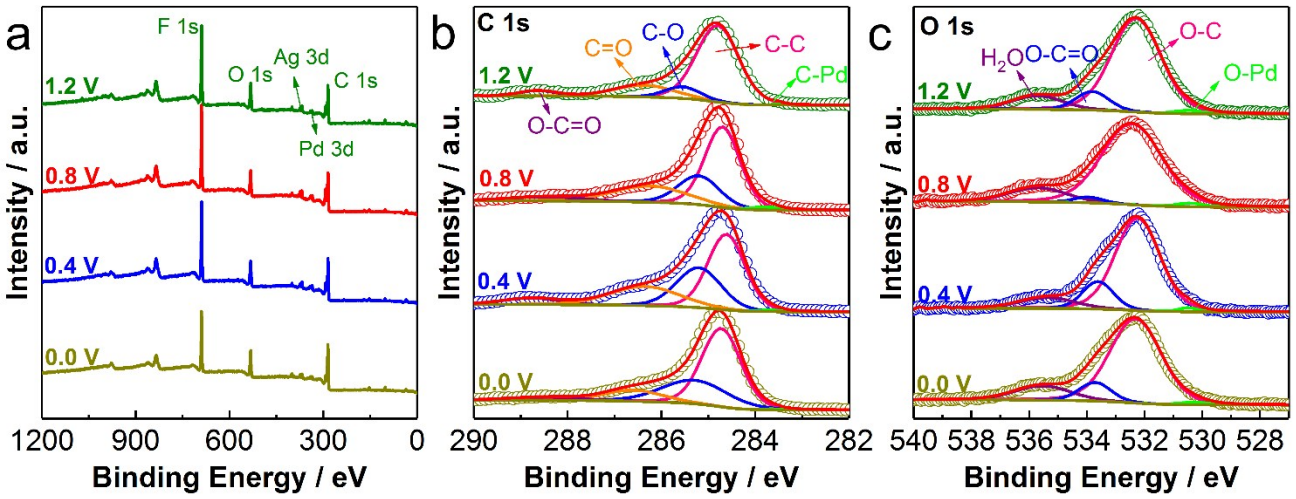

Fig. S15. XPS analysis of the $Ag_{49}Pd_{51}$/rGO catalyst after FOR test in N_2-saturated 1M KOH + 1 M HCOOK electrolyte at different upper limit potential of 0.0 V, 0.4 V, 0.8 V and 1.2 V with a scan rate of 50 mV s^{-1} for 10 cycles. (a) XPS survey spectra. (b, c) High-resolution spectra of C 1s and O 1s.

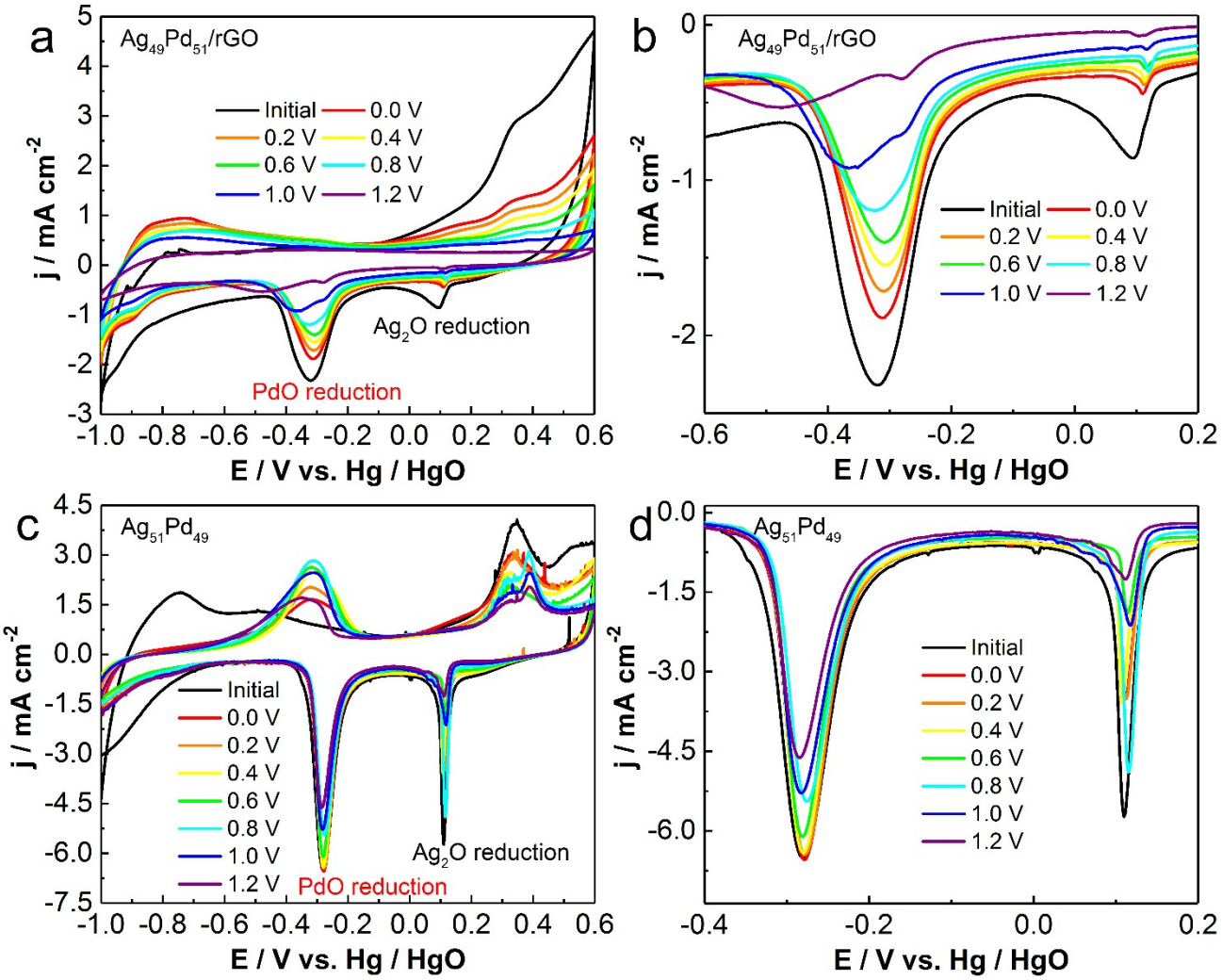

Fig. S16. (a) CV curves of $Ag_{49}Pd_{51}$/rGO catalyst in N_2-saturated 1 M KOH electrolyte taken before and after FOR test at different upper limit potential of 0.0, 0.2, 0.4, 0.6, 0.8, 1.0 and 1.2 V normalized with the area of glassy carbon (GC) electrode (0.196 cm^2). (b) Enlarged details of the PdO and Ag_2O reduction regions in (a). (c) CV curves of $Ag_{51}Pd_{49}$ nanoalloy in N_2-saturated 1 M KOH electrolyte taken before and after FOR test at different upper limit potential of 0.0, 0.2, 0.4, 0.6, 0.8, 1.0 and 1.2 V normalized with the area of glassy carbon (GC) electrode (0.196 cm^2). (d) Enlarged details of the PdO and Ag_2O reduction regions in (a). Unless indicated, all of the CV

tests were performed in N_2-saturated 1 M KOH + 1 M HCOOK electrolyte at a scan rate of 50 mV s^{-1}.

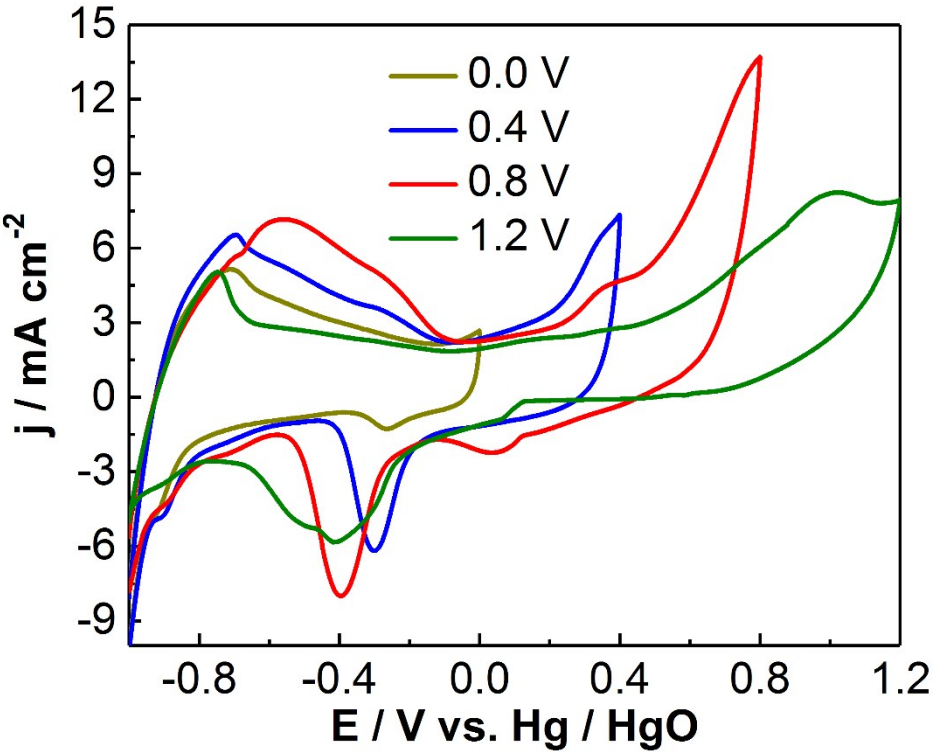

Fig. S17. (a) CV curves of $Ag_{49}Pd_{51}$/rGO catslyst in N_2-saturated 1 M KOH electrolyte taken after FOR test at different upper limit potential of 0.0, 0.4, 0.8 and 1.2 V at a scan rate of of 50 mV s^{-1} normalized with the area of glassy carbon (GC) electrode (0.196 cm^2).

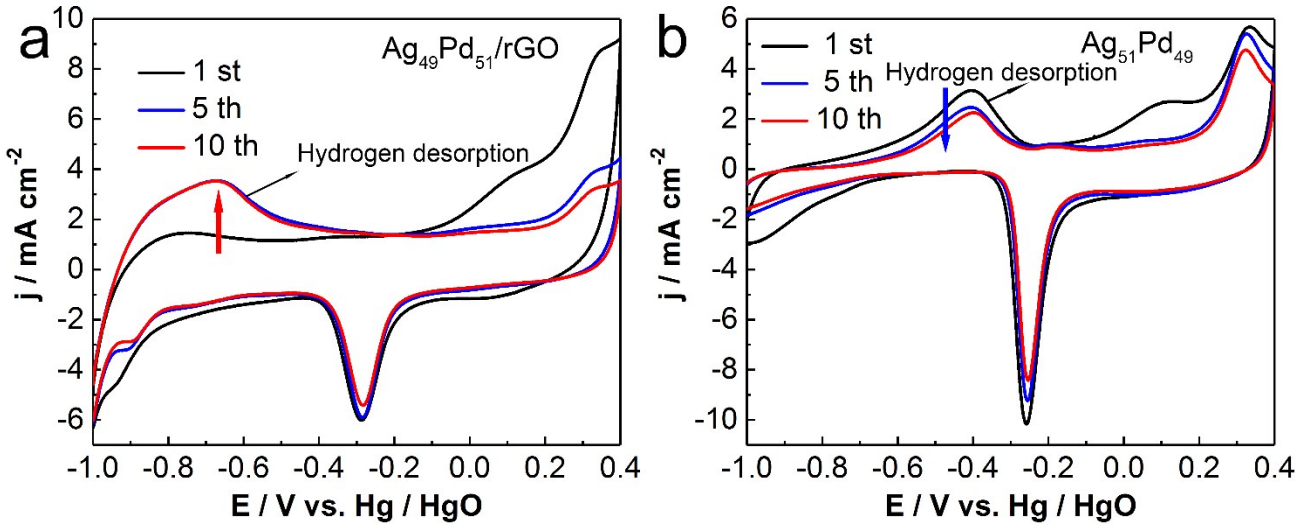

Fig. S18. CV curves of (a) $Ag_{49}Pd_{51}$/rGO and (b) $Ag_{51}Pd_{49}$ catalysts for the 1st, 5th and 10th cycles in N_2-saturated 1 M KOH electrolyte at a scan rate of of 50 mV s^{-1} normalized with the area of glassy carbon (GC) electrode (0.196 cm^2).

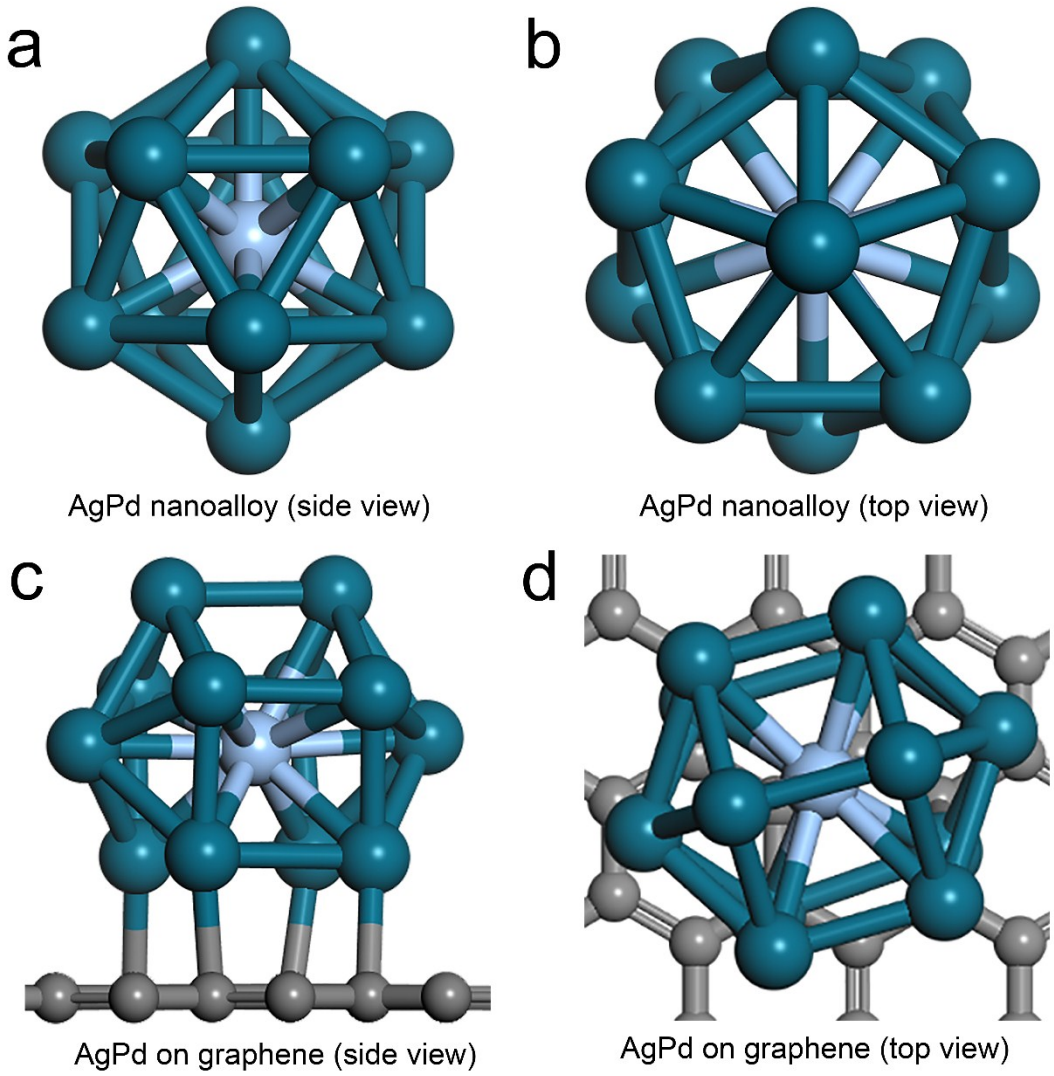

Fig. S19. (a, b) Geometry optimized model of AgPd nanoalloy on (a) side view and (b) top view. (c, d) Geometry optimized model of AgPd/graphene on (c) side view and (d) top view. The light-blue, dark-blue and gray balls represent the Ag, Pd and C atoms, respectively.

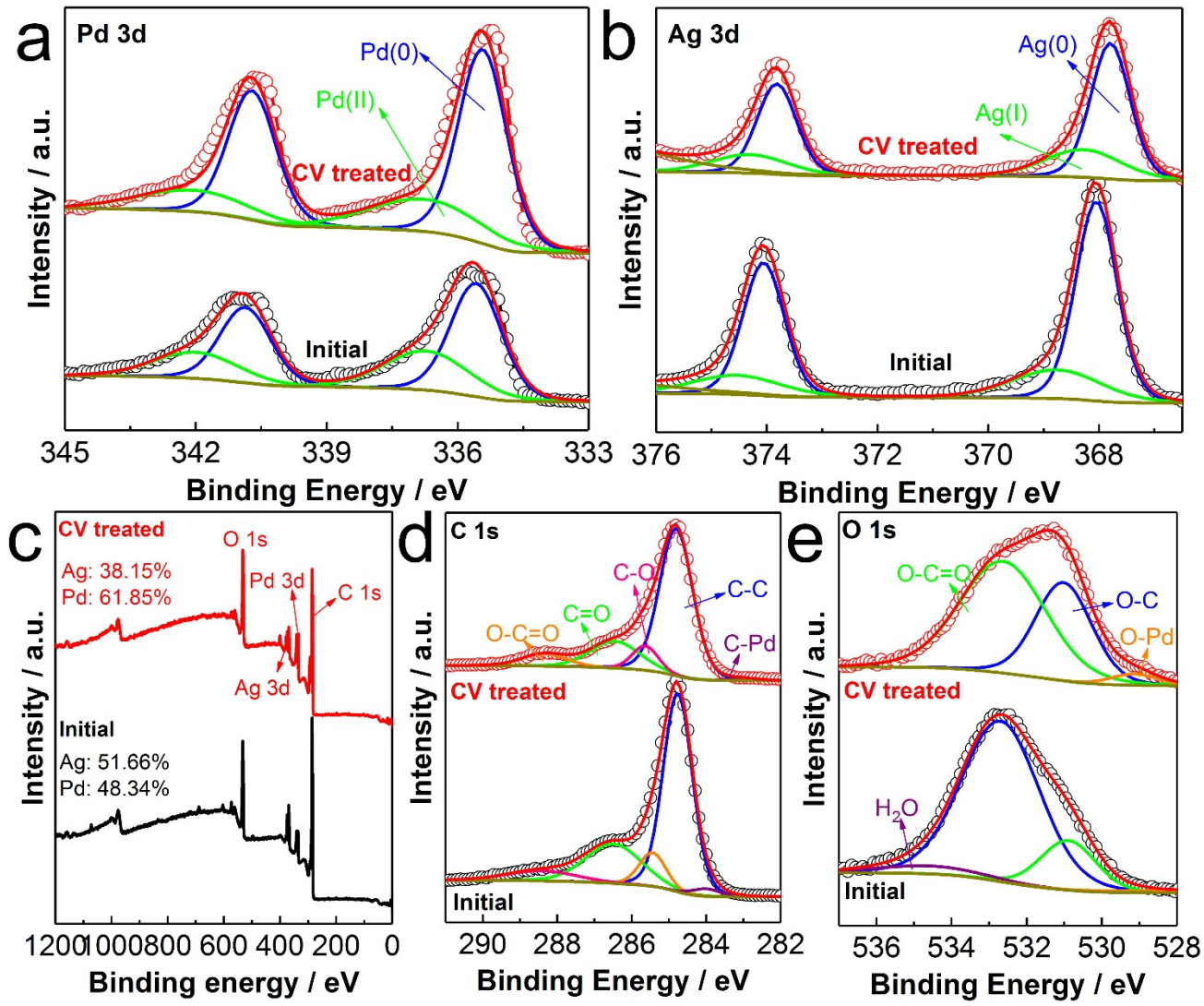

Fig. S20. XPS analysis of $Ag_{49}Pd_{51}$/rGO catalyst before and after CV in N_2-saturated 1M KOH electrolyte at an upper limit potential of 0.4 V with a scan rate of 50 mV s^{-1} for 10 cycles. (a, b) High-resolution spectra of Pd 3d and Ag 3d. (c) XPS survey spectra. (d, e) High-resolution spectra of C 1s and O 1s.

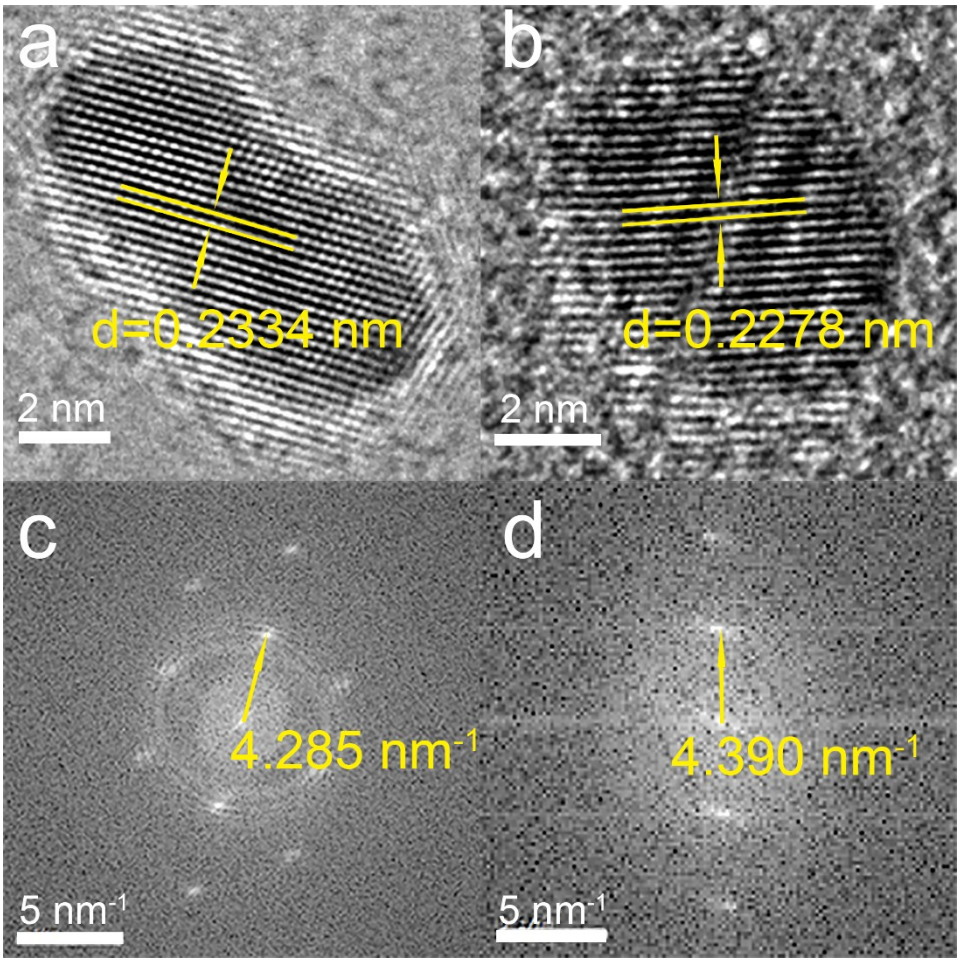

Fig. S21. HRTEM and corresponding FFT images of $Ag_{49}Pd_{51}$/rGO catalyst (a, c) before and (b, d) after CV in N_2-saturated 1M KOH electrolyte at upper limit potential of 0.4 V with a scan rate of 50 mV s^{-1} for 10 cycles.

Table S1. Mass fraction of Pd in the as-prepared catalysts measured by inductively coupled plasma optical emission spectrometer (ICP-OES).

	Mass [mg]	Volume [mL]	ID1 [mg mL^{-1}]	ID2 [mg mL^{-1}]	ID3 [mg mL^{-1}]	Mass fraction [%]
$Ag_{77}Pd_{23}$/rGO	13.1	53	17.79	17.83	16.68	**7.05**
$Ag_{49}Pd_{51}$/rGO	15.6	100	28.59	28.45	27.59	**18.08**
$Ag_{27}Pd_{73}$/rGO	15.8	100	33.44	33.74	32.87	**21.11**
Pd/rGO	9.9	100	22.53	22.53	21.17	**22.23**

Table S2. The position and fraction of various surface compositions in Ag 3d and Pd 3d for $Ag_{49}Pd_{51}$/rGO catalyst after FOR test at different upper limit potential of 0.0, 0.4, 0.8 and 1.2 V with a scan rate of 50 mV s^{-1} for 5 cycles.

Sample	Ag $3d_{3/2}$				Ag $3d_{5/2}$				Ag/(Ag+Pd) [%]
	Ag(0)		Ag(II)		Ag(0)		Ag(II)		
	Position [eV]	Fraction [%]	Position [eV]	Fraction [%]	Position [eV]	Fraction [%]	Position [eV]	Fraction [%]	
0.0 V	374.00	73.04	374.57	26.96	368.00	73.04	368.57	26.96	48.13
0.4 V	374.04	71.77	374.54	28.23	368.04	71.77	368.54	28.23	39.94
0.8 V	374.54	68.08	374.51	31.92	368.08	68.08	368.54	31.92	37.58
1.2 V	374.17	92.69	375.20	7.31	368.17	92.69	369.20	7.31	41.66

Sample	Pd $3d_{3/2}$				Pd $3d_{5/2}$				Pd/(Ag+Pd) [%]
	Pd(0)		Pd(II)		Pd(0)		Pd(II)		
	Position [eV]	Fraction [%]	Position [eV]	Fraction [%]	Position [eV]	Fraction [%]	Position [eV]	Fraction [%]	
0.0 V	340.77	60.14	341.93	39.86	335.47	60.14	336.63	39.86	51.87
0.4 V	340.83	59.31	341.93	40.69	335.53	59.31	336.68	40.69	60.06
0.8 V	340.83	58.94	342.07	41.06	335.53	58.94	336.77	41.06	62.42
1.2 V	340.78	59.64	341.91	40.36	335.47	59.64	336.61	40.36	58.34

Table S3. The position and fraction of various surface compositions in Ag 3d and Pd 3d for $Ag_{49}Pd_{51}$/rGO catalyst before and after CV in N_2-saturated 1M KOH electrolyte at an upper limit potential of 0.4 V with a scan rate of 50 mV s^{-1} for 10 cycles.

Sample	Ag $3d_{3/2}$				Ag $3d_{5/2}$				Ag/(Ag+Pd) [%]
	Ag(0)		Ag(II)		Ag(0)		Ag(II)		
	Position [eV]	Fraction [%]	Position [eV]	Fraction [%]	Position [eV]	Fraction [%]	Position [eV]	Fraction [%]	
Initial	374.06	76.08	374.53	23.92	368.05	76.08	368.76	23.92	51.66
CV treated	373.82	72.02	374.30	27.98	367.79	72.02	369.28	27.98	38.15

Sample	Pd $3d_{3/2}$				Pd $3d_{5/2}$				Pd/(Ag+Pd) [%]
	Pd(0)		Pd(II)		Pd(0)		Pd(II)		
	Position [eV]	Fraction [%]	Position [eV]	Fraction [%]	Position [eV]	Fraction [%]	Position [eV]	Fraction [%]	
Initial	340.86	63.54	341.99	36.46	335.58	63.54	336.71	36.46	48.34
CV treated	340.71	72.27	342.04	27.73	335.43	72.27	336.76	27.73	61.85